

Automated Detection of Diabetic Retinopathy in Fundus Images

Raju Maher², Sangramsing Kayte¹, Suvarnsing Bhable², Jaypalsing Kayte²

¹Dept. of Computer Science & IT, Dr. Babasaheb Ambedkar Marathwada University, Aurangabad, Maharashtra, India

²Department of Digital and Cyber Forensic, Aurangabad, Maharashtra, India

Abstract—

D iabetic retinopathy is one vascular disorder where the retina is damaged because fluid leaks from blood vessels into the retina. Early diagnosis of diabetic retinopathy enables timely treatment and in order to achieve it a major effort will have to be invested into screening programs and especially into automated screening programs. For automated screening programs to work robustly efficient image processing and analysis algorithms have to be developed. Candidates are detected using a combination of coarse and fine segmentation. The coarse segmentation is based on a local variation operation to outline the boundaries of all candidates which have clear borders. Using a clinician's reference for ground truth exudates were detected from a database with 89.7% sensitivity, 99.3% specificity and 99.4% accuracy. Due to its distinctive performance measures, the proposed method may be successfully applied to images of variable quality.

Keywords— diabetic retinopathy, image processing, image analysis, optic disk localization, blood vessel segmentation, microaneurysms, exudates, hemorrhages, neovascularization

I. INTRODUCTION

Diabetic retinopathy (DR) is one of the leading disabling chronic diseases, and one of the leading causes of preventable blindness in the world [1]. It was found to be the fourth most frequently managed chronic disease in general practice in 2009, and the projections go as high as the second most frequent disease by the year 2030 [1]. The global burden of diabetic patients is expected to rise from 171 million in 2000 to 366 million in 2030 [1]. In Europe more than 52.8 million people are diagnosed with diabetes with the number expected to rise to 64 million by 2030. In Croatia about 300 thousand people are estimated to have diabetes and of those only 190 thousand are registered. Early diagnosis of diabetic retinopathy enables timely treatment that can ease the burden of the disease on the patients and their families by maintaining a sufficient quality of vision and preventing severe vision loss and blindness [2]. In addition to the obvious medical benefits, significant positive economical effects are achieved by maintaining patient's workability and self-sustainability.

In order to achieve early diagnosis of diabetic retinopathy a major effort will have to be invested into screening programs. Screening is important as up to one third of people with diabetes may have progressive DR changes without symptoms of reduced vision [3], thus allowing the disease to progress and making treatment difficult. Systematic screening programs for diabetic eye disease have been developed in many countries [4], [5], [6]. In the UK, the NHS Diabetic Screening Program offers

annual fundus photography for all patients with diabetes over the age of 12, regardless of their socio-economic status [6]. In current screening programs only color fundus photography is used, and the data are sent to a grading center for reading where expert human readers estimate the disease severity. The main disadvantage is the necessity for qualified experts to grade the images, e.g. in the NHS Diabetes Screening Program one patient's images can be graded by up to four different experts. This standard is impossible to achieve in countries with a shortage of qualified medical personnel.

Fundus imaging has an important role in diabetic retinopathy detection and monitoring because eye fundus is sensitive to vascular diseases and we can consider fundus imaging as a candidate for non-invasive screening. The success of this type of screening approach depends on accurate fundus image capture, and especially on accurate and robust image processing and analysis algorithms for detection of abnormalities. Many algorithms have been proposed for fundus image analysis using different methods and approaches.

The main contribution of this work is to present an overview of algorithms for early detection of diabetic retinopathy in fundus photographs. In Section II typical symptoms of diabetic retinopathy are explained. In Section III an overview of image processing algorithms for early detection diabetic retinopathy is given. In Section IV currently available databases for image processing algorithms testing and evaluation are presented and finally in Section V we give a short conclusion.

II. DIABETIC RETINOPATHY

Diabetes is a well-known disease and may cause abnormalities in the retina (diabetic retinopathy), kidneys (diabetic nephropathy), nervous system (diabetic neuropathy) and is known to be a major risk for cardiovascular diseases. Diabetic retinopathy is a microvascular complication caused by diabetes which can lead to blindness. In early stages of diabetic retinopathy typically there are no visible signs but the number and severity of abnormalities increase during the time. Diabetic retinopathy typically starts with small changes in retinal capillaries. The first detectable abnormalities are microaneurysms which represent local enlargements of the retinal capillaries. The ruptured microaneurysms can cause hemorrhages. After a period of time, hard exudates may appear. The hard exudates are lipid formations leaking from

weakened blood vessels. As the retinopathy advances, the blood vessels may become obstructed which causes microinfarcts in the retina. These microinfarcts are called soft exudates. Extensive lack of oxygen caused by microinfarcts causes the development of new fragile vessels. This phenomenon is called neovascularization which is a serious eyesight threatening state and may cause sudden loss in visual acuity or even permanent blindness. Examples of microaneurysms, hemorrhages, hard exudates, soft exudates and neovascularization are visible in Fig. 1.

After diagnosis of diabetic retinopathy, regular monitoring is needed due to progressive nature of the disease. Sadly, broad screening cannot be performed due to the fact that fundus image examination requires medical experts. For the screening, automated image processing methods must be developed and to develop automated image processing methods high quality databases for algorithm evaluation are required.

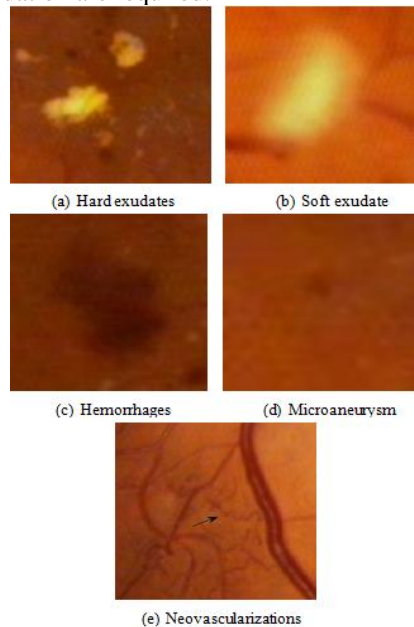


Fig. 1: Abnormal findings in the eye fundus images caused by diabetic retinopathy

III. STATE OF THE ART IMAGE PROCESSING ALGORITHMS

An overview of current state of art image processing algorithms known to us is given in this section. The algorithms were classified in terms of five basic image processing and decision making categories and associated subdivision as follows:

- 1) Pre-processing
- 2) Localization and segmentation of the optic disk
 - a) Characteristics of the optic disk
 - b) Optic disk localization
 - c) Optic disk segmentation
- 3) Segmentation of the retinal vasculature
 - a) Characteristics of the vasculature
 - b) Methods for segmentation of the retinal vasculature
- 4) Localization of the macula and fovea
 - a) Characteristics of the macula and fovea
 - b) Methods for localization of the macula and fovea
- 5) Localization and segmentation of retinopathy
 - a) Microaneurysms/hemorrhages
 - b) Exudates
 - c) Neovascularizations

A. Image preprocessing

The main objective of image preprocessing methods is to attenuate image variation by normalizing the original retinal image against a reference model. Variations typically arise within the same image (intra-image variability) as well as between images (inter-image variability) and to enable efficient image analysis it is necessary to compensate for this variability. Intra-image variations arise due to differences in light diffusion, the presence of abnormalities, variation in fundus reflectivity and fundus thickness. Inter-image variability is caused by factors including differences in cameras, illumination, acquisition angle and retinal pigmentation. The illumination component of a digital retinal photograph is characterized by gradual non-uniform spatial variations. A number of general-purpose techniques have been investigated for attenuating this variation. Early approaches investigated space-variant filtering schemes supporting locally adaptive contrast enhancements. Highpass filtering and mathematical modeling of the nonuniformity followed by subtraction of this component from the observed image have also been investigated for the correction of non-uniform illumination [7]. Several authors proposed image formation models for describing the observed retinal image, typically in terms of a

foreground image, background image and an acquisition transformation function [8], [9]. The foreground image contains the vasculature, optic disk and any visible lesions. The background image contains all illumination variation due to the transformation function of the original image. Shade-correction is a method in which the background image is first approximated by smoothing the original image with a mean or median filter whose size is larger than the largest retinal feature. The original image may then be divided by the filtered image or the filtered image subtracted from the original image [10]. In [11] authors apply alternation sequential filters to calculate the background approximation in order to avoid artifacts at borders of bright regions. In [12] a method was proposed for correcting the non-uniform illumination using a nonlinear point transformation to correct image intensity. In [13] authors used a parameterized model to normalize the output image. Color is a powerful descriptor with significant potential as a means of discriminating between retinal features. Early work [14] identified differences in the color of different types of lesions in color retinal images. Empirical research by several authors showed that the green channel of RGB images contains the maximum contrast [15], [16], [17]. Color normalization is required due to the significant intra-image and inter-image variability in the color of the retina in different patients. Recent work has investigated color normalization techniques for attenuating color variation. In [18] authors first transformed the original retinal image to an intensity-hue-saturation representation. This separation of different components allows the normalization of the intensity channel without changing the perceived relative color values of the pixels.

Histogram equalization redistributes the histogram of each color channel in the input image such that the output image contains a uniform pixel value distribution. The assumption is that for each color plane the pixel rank order is maintained even with variations in illumination. A monotonic, non-linear transformation function is applied to equalize the histogram of each separate color channel. An output image is produced by applying the function to map each gray level value in the input image to a new corresponding value in the output image. Histogram specification is an alternative form of histogram processing for color normalization. The distribution of each color channel is interpolated to more closely match that of a reference model. The reference model is usually obtained from an image selected by an expert to maximize the performance of automated detection techniques. Histogram specification is a two-stage process. First, the histogram of each channel is equalized and then an inverse transformation function is applied to determine the desired histogram for each color channel in the output image. In [19] authors applied histogram specification in order for all the sample images to match a reference image distribution. Contrast enhancement methods are aimed at altering the visual appearance that makes an object distinguishable from other objects and the background. In literature number of methods for contrast enhancement are described. Retinal images acquired using standard clinical protocols often exhibit low contrast. In [20], [21] authors reported that retinal images typically have a higher contrast in the center of the image with reduced contrast moving outward from the center. Contrast manipulation is usually done in two steps in which a local contrast enhancement step is followed by a noise reduction step. Those methods use small windows as local transforms after correcting for non-uniform illumination. In [18] authors proposed an adaptive contrast enhancement transformation which depends on the mean and variance of the intensity within a local region. The transformation operation is applied to the intensity component of an HSI representation of the image which has been smoothed to attenuate background noise. This adaptive transformation provides a large increase in contrast in regions with an initially small variance and little contrast enhancement for an initially large variance. In [17] authors proposed a multilevel histogram equalization method as a preprocessing step in the detection of drusen. The approach is based on the sequential application of histogram equalization to progressively smaller non-overlapping neighborhoods.

B. Localization and segmentation of the optic disk

The optic disk is the visible part of the optic nerve head within the retina. The optic disk is generally brighter than the surrounding area with an elliptical contour. Variation in pigmentation within normal eyes causes differences in appearance of the disk. Many vessels crossing the optic disk can be typically seen in fundus photographs. Localization of the optic disk is often necessary to differentiate the disk from other features of the retina like exudates, cotton wool spots and as an important landmark.

1) Optic disk localization: Optic disk localization consist mainly of finding the approximate center of the optic disk or placing the disk within a specific region such as a circle or square. In either way, many distractors like blood vessel edges or large exudate lesions complicate the process of optic disk localization. In early papers the optic disk was localized by identifying the largest cluster of bright pixels [22]. Algorithms which rely solely on intensity variation proved to be simple, fast and reasonably robust for optic disk localization in normal retina images without many pathologies but in cases where many yellow/white lesions exist these simple methods may fail.

Many authors used characteristics of the optic disk like intensity, morphology and color for optic disk localization. In [18] authors used an 80×80 pixel sub-image to evaluate the intensity variance of adjacent pixels. The point with the largest variance was assumed to be centre of the optic disk. The author reported sensitivity of 99.1% in localization of optic disk in images with little or no signs of white lesions.

The Hough transform has been investigated by a number of authors for the localization of the optic disk [23], [24], [25], [26], [27]. In [25] authors for example used a circular Hough transform after edge detection to localize the optic disks in the red color channel. The first stage searched for an optic disk candidate region defined as a 180×180 pixel region that included the brightest 2% of gray level values. A Sobel operator was applied to detect the edge points of the candidate region and the contours were then detected by means of the circular Hough transform.

Principle component analysis has also been used as a means of extracting common features of retinal images including the optic disk and blood vessels [28], [29]. The likelihood of a candidate region being an optic disk was determined by

comparing the characteristics of the optic disk extracted from a training image to those derived from an unseen image. In [28] authors reported the correct localization of the optic disk in 99% of 89 images.

In [30] authors proposed a pyramidal decomposition technique in combination with Hausdorff-based template matching. First, potential regions containing the optic disk were located by means of a pyramidal decomposition of the green channel image. Next, the optic disk was localized using the Hausdorff distance to compare the candidate region to a circular template with dimensions approximating the optic disk. Authors reported correct localization of the optic disk in 40 of 40 images.

In [31] authors proposed a vessel tracking technique to trace the parent–child relationship between blood vessel segments towards a point of convergence assumed be the centre of the optic disk. Authors in [32] also proposed the convergence of blood vessels as a means of localizing the center of the optic disk. The approach correctly identified the optic disk location in 89% of 81 images, 50 of which were diseased retinas. In [9] authors localized the optic disk by fitting a parametric geometrical model of the retinal vascular system to the main vessels extracted from the image. The vascular structure is first segmented to provide accurate measurements of the vessel center point position, diameter and direction. The geometrical model of the retina is then fitted to the main vessels within the image to localize the center of the optic disk.

2) Optic disk segmentation: Optic disk segmentation is usually performed after optic disk localization. There are many algorithms for determining the disk contour. In [33] authors describe an approach using color space transformation and morphological filtering techniques for disk localization. The optic disk was first localized using the luminance channel of the HLS color space and a thresholding operation was applied to determine the approximate locus of the optic disk. The precise contour of the disk was then determined, using the red channel of the RGB color space, via a watershed transform. Active contours or snakes have been investigated by several authors for optic disk segmentation. Early work [34] exploited an active contour to determine the boundary of the optic disk. However, a quantitative assessment of the approach was not presented in the paper. In [35] authors investigated applying a morphological operator followed by an active contour to segment the disk. A dilation operator was first applied, followed by an erosion operator to re-establish the optic disk contour. Finally, a morphological reconstruction operator was applied by maintaining the maximum of the dilated/eroded image and the original one. After that an active contour was initialized as a circle centered on and inside the optic disk. The contour was fitted to the edge of the disk using the gradient vector flow (GVF) technique. In [36] authors proposed a two stage extension to improve the performance of GVF snakes for optic disk segmentation. The optic disk was first localized using template matching and after that color morphological processing was used to obtain a more homogeneous inner disk area in order to increase the accuracy of the snake initialization. Authors in [20] used a similar two stage process for optic disk segmentation. First authors used template matching for optic disk localization and after that a specialized three phase elliptical global and local deformable model with variable edge-strength dependent stiffness was then fitted to the contour of the disk.

C. Segmentation of the retinal vasculature

The segmentation of the retinal vasculature is very important because retinal vasculature contains many useful information about the patients health. Accurate segmentation of the retinal blood vessels is often an essential prerequisite step in the identification of the retinal anatomy and pathology. Segmentation of blood vessels is important for image registration or spatial alignment of images.

The retinal vasculature is composed of arteries and veins. The central retinal artery bifurcates at or on the optic disk into divisions that supply the four quadrants of the inner retinal layers. The vessels have a lower reflectance compared to other retinal surfaces and because of that they appear darker relative to the background. Occasionally a light streak running the length of the vessel is reflected from the transparent convex wall of the arteriole. There are many different algorithms for segmentation of blood vessels.

Matched filtering for the detection of the vasculature convolves a 2D kernel with the retinal image. In [22] authors proposed a two-dimensional linear kernel with a Gaussian profile for segmentation of the vasculature. The profile of the filter is designed to match that of a blood vessel, which typically has a Gaussian or a Gaussian derivative profile. The kernels are typically rotated in 30–45 degree increments to fit into vessels of different orientations. The highest response filter is selected for each pixel and is typically thresholded to provide a vessel image. Further post processing is then applied to identify vessel segments. Matched filtering performs well when used in conjunction with additional processing techniques but there are some problems. Convolution kernels may be quite large and need to be applied in several orientations which can be very computationally expensive. Kernel responds optimally to vessels that have the same standard deviation of the underlying Gaussian function specified by the kernel. Retinal background and low contrast of smaller vessels increase the number of false responses around bright objects. Several authors have proposed refinements and extensions which address many of these problems [37],[38].

Morphological operators have been applied for vasculature segmentation [39] because the basic morphology of the vasculature is known a priori to be comprised of connected linear segments and because of speed and noise resistance.

Vessel tracking algorithms segment a vessel between two points. A vessel tracking algorithm typically steps along the vessel. The center of the longitudinal crosssection of vessel is determined with various properties of the vessel including average width and tortuosity measured during tracking. The main advantage of vessel tracking methods is that they provide highly accurate vessel widths, and can provide information about individual vessels that is usually unavailable using other methods. Unfortunately, they require the starting point and sometimes vesseltracking techniques may be confused by vessel crossings and bifurcations. Many authors experimented with vessel tracking algorithms [40].

Several authors have investigated a number of classification methods for the segmentation of the vessels. Artificial neural networks have been extensively investigated for segmentation of retinal vasculature [31] making classification based on statistical probabilities rather than objective reasoning. Radial projections with SVM were proposed in [41]. In [42] authors proposed multiscale Gabor filters as features and Gaussian Mixture Models for classification.

D. Localization of the fovea and the macula

Temporal to the optic nerve head is the macula which appears darker in color and has no blood vessels present in the center. The fovea lies at the center of the macula and is the part of the retina that is used for fine vision. Retinopathy in this area, termed maculopathy, is associated with a high risk of visual loss. The macula is a dark approximately circular area, but the contrast is often quite low and it may be obscured somewhat by exudates or hemorrhages. The fovea is located approximately 2–2.5 disk diameters temporal to the temporal edge of the optic disk and between the major temporal retinal vascular arcades [43]. These positional constraints can be used to identify a small search area for the macula. The detection of the macula and fovea is mainly determined by estimating the position in relation to other retinal features [44].

E. Localization and segmentation of retinopathy

In this subsection we give an outline of state of the art image processing algorithms for diabetic retinopathy pathologies detection.

1) Detection of microaneurysms/hemorrhages: Early work in automated detection of pathologies investigated fluorescein angiography images. In [10] authors proposed a morphological transformation to segment micro-aneurysms within fluorescein angiograms. The shade-corrected image was first opened by applying an erosion operator followed by dilation. An 11-pixel linear kernel was then applied in eight rotational orientations that, when combined, included all of the vessel sections and excluded all the circular microaneurysms. This opened image was extracted from the original shade-corrected image using a top-hat transformation producing an image that only contained microaneurysms. The authors reported a sensitivity of 82% and specificity of 86% in comparison to a clinician, with 100 false positive pixels per image reported.

In [45] authors proposed a method for the detection of microaneurysms in red-free images. The images were initially processed by shade correction of the image, followed by removal of vessels and other distractors by the top-hat transformation. A Gaussian matched filter was applied to retain candidate microaneurysms for subsequent classification. The classification algorithm was based on 13 different parameters derived from a training set of 102 images of variable degrees of retinopathy. The parameters included shape, intensity, circularity, perimeter length and length ratio. The study used a total of 3783 images from 589 patients on 977 visits. The images were graded for presence/absence of microaneurysms and/or hemorrhages against the reference standard of an experienced clinical research fellow.

In [46] the green channel of the image was inverted and smoothed with a Gaussian filter. A set of scan lines with equidistantly sampled tangents between -90 and +90 was fixed. For each direction the intensity values along the scan lines were recorded in a one dimensional array, and the scan lines were shifted vertically and horizontally to process every image pixel of the image. On each intensity profile, the heights of the peaks, and their local maximum positions were used for adaptive thresholding. The resulting foreground indices of the thresholding process were transformed back to two dimensional coordinates, and stored in a map that records the number of foreground pixels of different directions corresponding to every position of the image. The maximal value for each position equals the number of different directions used for the scanning process. This map was smoothed with an averaging kernel and a hysteresis thresholding procedure was applied. The resulting components were filtered based on their size.

In order to extract candidates, authors in [47] constructed a maximal correlation response image for the input retinal image. This was accomplished by considering the maximal correlation coefficient with five Gaussian masks with different standard deviations for each pixel. The maximal correlation response image was thresholded with a fixed threshold value to obtain the candidates. Vessel detection and region growing was applied to reduce the number of candidates, and to determine their precise size, respectively.

A number of authors investigated neural networks for detection of microaneurysms and hemorrhages [48], [49].

In [50] authors presented a method which combines outputs of different state of the art microaneurysm candidate extractors. They applied simulated annealing to select an optimal combination of such algorithms for particular dataset.

Morphological processing algorithms are the most commonly used algorithms for hemorrhage detection. In [51] authors presented a spot lesion detection algorithm using multiscale morphological processing. Blood vessels and over-detection were removed by scale-based lesion validation. An algorithm was tested on 30 retinal images and it achieved the sensitivity and predictive value of 84.10% and 89.20% respectively. In [52] watershed algorithm was used for segmentation of splats, a collection of pixels with similar color and spatial location. The connected vasculatures were removed by automated vessels segmentation method. The kNN classifier was applied with 42 features in training and reduced to 7 features using forward feature selection method in testing stage. A hybrid method for hemorrhage detection was presented in [53]. Hemorrhage candidates were extracted using a circular shaped template matching with normalized crosscorrelation. Then hemorrhages were segmented by two methods of region growing: region growing segmentation using the local threshold and adaptive seed region growing segmentation.

2) Exudate detection: Many attempts to detect exudate lesions can be found in the literature. Exudates detection and identification was first investigated in [54]. Global and local thresholding values were used to segment exudate lesions and reported a sensitivity of 61% and 100% based on 14 images. Some works use the high luminosity of exudates to separate them from the background by thresholding. Edge detectors, combined with other techniques, have been applied

in several studies to extract the borders of exudates. Other authors have examined the ability of Bayesian classifiers to detect retinal lesions. A Bayesian classifier has also been used to identify candidate red and bright lesions, which were subsequently classified into the right type of lesion using a supervised method [55]. A k-nearest neighbors algorithm, together with a static classifier combination scheme, has been used as well to determine whether a retinal image contains exudates [56]. The differentiation of exudates from cotton wools and drusen has been addressed using an approach based on k-nearest neighbors and linear discriminant analysis classifier [57]. The use of Fisher's linear discriminant and Kirsch operator to detect exudates on the basis of their color and the sharpness of their edges has also been reported [58]. Mixture models have been also investigated with this purpose. Other approaches are based on neural network (NN) classifiers, like multilayer perceptrons (MLPs) and support vector machines (SVMs) [59].

3) Detection of neovascularization: Neovascularization is a serious eyesight threatening state and may cause sudden loss in visual acuity or even permanent blindness and because of that it is very important to detect signs of neovascularization in fundus photographs. In [60] authors a various combination of techniques such as image normalization, compactness classifier, morphology-based operator, Gaussian filtering and thresholding techniques were used in developing neovascularization detection algorithms.

IV. PUBLICLY AVAILABLE RETINAL IMAGE DATABASES

Image databases are very important because all image processing algorithms developed have to be tested and verified. An overview of all publicly available retinal image databases known to us is given in this section.

A. DRIVE database

The DRIVE (Digital Retinal Images for Vessel Extraction) is a publicly available database, consisting of a total of 40 color fundus photographs [61]. Each image has been JPEG compressed. Of the 40 images in the database, 7 contain pathology, namely exudates, hemorrhages and pigment epithelium changes. The images were acquired using a Canon CR5 non-mydratic 3-CCD camera with a 45° field of view (FOV). Each image was captured using 8 bits per color plane at 768×584 pixels. The FOV of each image was circular with a diameter of approximately 540 pixels.

B. STARE database

The STARE database contains 20 images for blood vessel segmentation; ten of these contain pathology [62]. The slides were captured by a Topcon TRV-50 fundus camera at 35° field of view. Each slide was digitized to produce a 605×700 pixel image, 24 bits per pixel (standard RGB). Two observers manually segmented all the images.

C. ARIA online

This database was created in 2006, in a research collaboration between St. Paul's Eye Unit, Royal Liverpool University Hospital Trust, Liverpool, UK and the Department of Ophthalmology, Clinical Sciences, University of Liverpool, Liverpool, UK [63]. The trace of blood vessels, the optic disc and fovea location was marked by two image analysis experts as the reference standard. The images were captured at a resolution of 768×576 pixels in RGB color with 8-bits per color plane with a Zeiss FF450+ fundus camera at a 50° FOV and stored as uncompressed TIFF files.

D. ImageRet

The ImageRet database was made publicly available in 2008 and is subdivided into two sub-databases, DIARETDB0 and DIARETDB1 [64]. DIARETDB0 contains 130 retinal images of which 20 are normal and 110 contain various signs of diabetic retinopathy. DIARETDB1 contains 89 images out of which 5 images represent healthy retinas while the other 84 have some diabetic retinopathy signs. The images were acquired with a 50° FOV using a fundus camera at a size of 1500×1152 pixels in PNG format. The images were annotated by four experts for the presence of microaneurysms, hemorrhages, and hard and soft exudates. Annotated images from four experts were combined to produce a single ground truth image.

E. Messidor

The Messidor-project database, with 1200 retinal images, is the largest database currently available on the Internet and is provided by the Messidor program partners [65]. The images were acquired by 3 ophthalmologic departments using a color video 3CCD camera on a Topcon TRC NW6 non-mydratic camera with a 45° FOV. The images were captured using 8 bits per color plane at 1440×960, 2240×1488, or 2304×1536 pixels. 800 images were acquired with pupil dilation and 400 without dilation. The reference standard provided contains the grading for diabetic retinopathy and the risk of macular edema in each image.

F. Review

The Retinal Vessel Image set for Estimation of Widths (REVIEW) was made available online in 2008 by the Department of Computing and Informatics at the University of Lincoln, Lincoln, UK [66]. The dataset contains 16 mydratic images with 193 annotated vessel segments consisting of 5066 profile points manually marked by three independent experts.

G. ROC microaneurysm set

The Retinopathy Online Challenge microaneurysm dataset is part of a multi-year online competition of microaneurysm detection that was arranged by the University of Iowa in 2009 [67]. The set of data used for the competition consisted of 50 training images with available reference standard and 50 test images where the reference standard was withheld by the

organizers. The images were captured using a Topcon NW100, a Topcon NW200 or a Canon CR5-45NM non-mydiatic camera at 45 ° FOV and were JPEG compressed in the camera. There are three different image sizes present in the database; 768×576 , 1058×1061 and 1389×1383 pixels.

H. HEI-MED

The Hamilton Eye Institute Macular Edema Dataset (HEI-MED) is a collection of 169 fundus images to train and test image processing algorithms for the detection of exudates and diabetic macular edema [68]. The dataset is composed of 169 JPEG images compressed at highest quality. Each image of the dataset was manually segmented by Dr. Edward Chaum (an expert ophthalmologist from HEI). He identified all the exudation areas and other bright lesions such as cotton wool spots, drusens or clearly visible fluid occurring on the fundus.

I. DRiDB

Diabetic Retinopathy Image Database is a new database developed in cooperation between Faculty of Electrical Engineering and Computing, University of Zagreb and Clinical Hospital Center “Sestre Milosrdnice” from Zagreb [69]. The images were captured at a resolution of 720×576 pixels in RGB color with 8-bits per color plane with a Zeiss VISUCAM 200 fundus camera at a 45 ° FOV and stored as uncompressed BMP files. A set of ground truth images accompanies every color fundus image from the database. For each image from the database five experts independently marked diabetic retinopathy findings (microaneurysms, hemorrhages, hard exudates, soft exudates). The experts were asked to mark the blood vessels, optic disc and macula alongside marked diabetic retinopathy findings and finally experts performed annotation of neovascularizations.

V. CONCLUSION

Early detection of diabetic retinopathy is very important because it enables timely treatment that can ease the burden of the disease on the patients and their families by maintaining a sufficient quality of vision and preventing severe vision loss and blindness. Positive economical benefits can be achieved with early detection of diabetic retinopathy because patients can be more productive and can live without special medical care. Image processing and analysis algorithms are important because they enable development of automated systems for early detection of diabetic retinopathy. In this paper we gave a short overview of major image processing components required to build an automated system for early detection of diabetic retinopathy.

REFERENCES

- [1] S. Wild, G. Roglic, A. Green, R. Sicree, and H. King, “Global prevalence of diabetes: estimates for the year 2000 and projections for 2030,” *Diabetes Care*, vol. 27, no. 5, pp. 1047–1053, 2004.
- [2] S. J. Lee, C. A. McCarty, H. R. Taylor, and J. E. Keeffe, “Costs of mobile screening for diabetic retinopathy: a practical framework for rural populations,” *Aust J Rural Health*, vol. 9, no. 4, pp. 186–192, 2001.
- [3] C. A. McCarty, C. W. Lloyd-Smith, S. E. Lee, P. M. Livingston, Y. L. Stanislavsky, and H. R. Taylor, “Use of eye care services by people with diabetes: the Melbourne Visual Impairment Project,” *Br J Ophthalmol*, vol. 82, no. 4, pp. 410–414, 1998.
- [4] D. A. Askew, L. Crossland, R. S. Ware, S. Begg, P. Cranstoun, P. Mitchell, and C. L. Jackson, “Diabetic retinopathy screening and monitoring of early stage disease in general practice: design and methods,” *Contemp Clin Trials*, vol. 33, no. 5, pp. 969–975, 2012.
- [5] H. C. Looker, S. O. Nyangoma, D. Cromie, J. A. Olson, G. P. Leese, M. Black, J. Doig, N. Lee, R. S. Lindsay, J. A. McKnight, A. D. Morris, S. Philip, N. Sattar, S. H. Wild, and H. M. Colhoun, “Diabetic retinopathy at diagnosis of type 2 diabetes in Scotland,” *Diabetologia*, vol. 55, no. 9, pp. 2335–2342, 2012.
- [6] T. Peto and C. Tadros, “Screening for diabetic retinopathy and diabetic macular edema in the United Kingdom,” *Curr. Diab. Rep.*, vol. 12, no. 4, pp. 338–345, 2012.
- [7] R. C. Gonzalez and E. Richard, “Woods, digital image processing,” ed: Prentice Hall Press, ISBN 0-201-18075-8, 2002.
- [8] M. J. Cree, J. A. Olson, K. C. McHardy, P. F. Sharp, and J. V. Forrester, “The preprocessing of retinal images for the detection of fluorescein leakage,” *Physics in medicine and biology*, vol. 44, no. 1, p. 293, 1999.
- [9] M. Foracchia, E. Grisan, and A. Ruggeri, “Detection of optic disc in retinal images by means of a geometrical model of vessel structure,” *Medical Imaging, IEEE Transactions on*, vol. 23, no. 10, pp. 1189–1195, 2004.
- [10] T. Spencer, J. A. Olson, K. C. McHardy, P. F. Sharp, and J. V. Forrester, “An image-processing strategy for the segmentation and quantification of microaneurysms in fluorescein angiograms of the ocular fundus,” *Computers and biomedical research*, vol. 29, no. 4, pp. 284–302, 1996.
- [11] T. Walter, J.-C. Klein, P. Massin, and A. Erginay, “A contribution of image processing to the diagnosis of diabetic retinopathy-detection of exudates in color fundus images of the human retina,” *Medical Imaging, IEEE Transactions on*, vol. 21, no. 10, pp. 1236–1243, 2002.
- [12] Y. Wang, W. Tan, and S. C. Lee, “Illumination normalization of retinal images using sampling and interpolation,” in *Medical Imaging 2001*. International Society for Optics and Photonics, 2001, pp. 500–507.
- [13] M. Foracchia, E. Grisan, and A. Ruggeri, “Luminosity and contrast normalization in retinal images,” *Medical Image Analysis*, vol. 9, no. 3, pp. 179–190, 2005.
- [14] M. Goldbaum, N. Katz, M. Nelson, and L. Haff, “The discrimination of similarly colored objects in computer images of the ocular fundus.” *Investigative ophthalmology & visual science*, vol. 31, no. 4, pp. 617–623, 1990.

- [15] D. S. Shin, N. B. Javornik, and J. W. Berger, "Computer-assisted, interactive fundus image processing for macular drusen quantitation," *Ophthalmology*, vol. 106, no. 6, pp. 1119–1125, 1999.
- [16] J. J. Leandro, J. V. Soares, R. M. Cesar Jr, and H. F. Jelinek, "Blood vessels segmentation in nonmydriatic images using wavelets and statistical classifiers," in *Computer Graphics and Image Processing*, 2003. SIBGRAPI 2003. XVI Brazilian Symposium on. IEEE, 2003, pp. 262–269.
- [17] K. Rapantzikos, M. Zervakis, and K. Balas, "Detection and segmentation of drusen deposits on human retina: Potential in the diagnosis of age-related macular degeneration," *Medical image analysis*, vol. 7, no. 1, pp. 95–108, 2003.
- [18] C. Sinthanayothin, J. F. Boyce, H. L. Cook, and T. H. Williamson, "Automated localisation of the optic disc, fovea, and retinal blood vessels from digital colour fundus images," *British Journal of Ophthalmology*, vol. 83, no. 8, pp. 902–910, 1999.
- [19] A. Osareh, M. Mirmehdi, B. Thomas, and R. Markham,
- [20] "Automated identification of diabetic retinal exudates in digital colour images," *British Journal of Ophthalmology*, vol. 87, no. 10, pp. 1220–1223, 2003.
- [21] J. Lowell, A. Hunter, D. Steel, A. Basu, R. Ryder, E. Fletcher, and L. Kennedy, "Optic nerve head segmentation," *Medical Imaging, IEEE Transactions on*, vol. 23, no. 2, pp. 256–264, 2004.
- [22] D. Usher, M. Dumskyj, M. Himaga, T. Williamson, S. Nussey, and J. Boyce, "Automated detection of diabetic retinopathy in digital retinal images: a tool for diabetic retinopathy screening," *Diabetic Medicine*, vol. 21, no. 1, pp. 84–90, 2004.
- [23] S. Chaudhuri, S. Chatterjee, N. Katz, M. Nelson, and M. Goldbaum, "Detection of blood vessels in retinal images using two-dimensional matched filters," *IEEE Transactions on medical imaging*, vol. 8, no. 3, pp. 263–269, 1989.
- [24] M. Yulong and X. Dingru, "Recognizing the glaucoma from ocular fundus image by image analysts," in *Engineering in Medicine and Biology Society*, 1990., *Proceedings of the Twelfth Annual International Conference of the IEEE*. IEEE, 1990, pp. 178–179.
- [25] A. Pinz, S. Bernogger, P. Datlinger, and A. Kruger, "Mapping the human retina," *Medical Imaging, IEEE Transactions on*, vol. 17, no. 4, pp. 606–619, 1998.
- [26] Z. Liu, C. Opas, and S. M. Krishnan, "Automatic image analysis of fundus photograph," in *Engineering in Medicine and Biology Society*, 1997. *Proceedings of the 19th Annual International Conference of the IEEE*, vol. 2. IEEE, 1997, pp. 524–525.
- [27] B. Kochner, D. Schuhmann, M. Michaelis, G. Mann, and K.-H. Englmeier, "Course tracking and contour extraction of retinal vessels from color fundus photographs: Most efficient use of steerable filters for model-based image analysis," in *Proceedings of the SPIE Conference on Medical Imaging*, vol. 3338, 1998, pp. 755–761.
- [28] B. M. Ege, O. K. Hejlesen, O. V. Larsen, K. Møller, B. Jennings, D. Kerr, and D. A. Cavan, "Screening for diabetic retinopathy using computer based image analysis and statistical classification," *Computer methods and programs in biomedicine*, vol. 62, no. 3, pp. 165–175, 2000.
- [29] H. Li and O. Chutatape, "Automated feature extraction in color retinal images by a model based approach," *Biomedical Engineering, IEEE Transactions on*, vol. 51, no. 2, pp. 246–254, 2004.
- [30] C. I. Sanchez, R. Hornero, M. I. Lopez, and J. Poza, "Retinal image analysis to detect and quantify lesions associated with diabetic retinopathy," in *Engineering in Medicine and Biology Society*, 2004. *IEMBS'04. 26th Annual International Conference of the IEEE*, vol. 1. IEEE, 2004, pp. 1624–1627.
- [32] M. Lalonde, M. Beaulieu, and L. Gagnon, "Fast and robust optic disc detection using pyramidal decomposition and hausdorff-based template matching," *Medical Imaging, IEEE Transactions on*, vol. 20, no. 11, pp. 1193–1200, 2001.
- [33] K. Akita and H. Kuga, "A computer method of understanding ocular fundus images," *Pattern recognition*, vol. 15, no. 6, pp. 431–443, 1982.
- [34] A. Hoover and M. Goldbaum, "Locating the optic nerve in a retinal image using the fuzzy convergence of the blood vessels," *Medical Imaging, IEEE Transactions on*, vol. 22, no. 8, pp. 951–958, 2003.
- [35] T. Walter and J.-C. Klein, "Segmentation of color fundus images of the human retina: Detection of the optic disc and the vascular tree using morphological techniques," in *Medical Data Analysis*. Springer, 2001, pp. 282–287.
- [37] S. Lee and M. Brady, "Integrating stereo and photometric stereo to monitor the development of glaucoma," *Image and Vision Computing*, vol. 9, no. 1, pp. 39–44, 1991.
- [38] F. Mendels, C. Heneghan, P. Harper, R. Reilly, and J.-P. Thiran, "Extraction of the optic disk boundary in digital fundus images," in *Proc. 1st Joint BMES/EMBS Conf*, 1999, p. 1139.
- [39] A. Osareh, M. Mirmehdi, B. Thomas, and R. Markham, "Colour morphology and snakes for optic disc localisation," in *The 6th medical image understanding and analysis conference*. BMVA Press, 2002, pp. 21–24.
- [40] B. Zhang, L. Zhang, L. Zhang, and F. Karray, "Retinal vessel extraction by matched filter with first-order derivative of gaussian," *Computers in biology and medicine*, vol. 40, no. 4, pp. 438–445, 2010.

- [41] J. Odstrcilík, J. Jan, J. Gazarek, and R. Kolařík, "Improvement of vessel segmentation by matched filtering in colour retinal images," in World Congress on Medical Physics and Biomedical Engineering, September 7-12, 2009, Munich, Germany. Springer, 2009, pp. 327–330.
- [42] F. Zana and J.-C. Klein, "A multimodal registration algorithm of eye fundus images using vessels detection and hough transform," *Medical Imaging, IEEE Transactions on*, vol. 18, no. 5, pp. 419–428, 1999.
- [43] Y. Yin, M. Adel, and S. Bourennane, "Retinal vessel segmentation using a probabilistic tracking method," *Pattern Recognition*, vol. 45, no. 4, pp. 1235–1244, 2012.
- [44] X. You, Q. Peng, Y. Yuan, Y.-m. Cheung, and J. Lei, "Segmentation of retinal blood vessels using the radial projection and semi-supervised approach," *Pattern Recognition*, vol. 44, no. 10, pp. 2314–2324, 2011.
- [45] A. Osareh and B. Shadgar, "Automatic blood vessel segmentation in color images of retina," *Iran. J. Sci. Technol. Trans. B: Engineering*, vol. 33, no. B2, pp. 191–206, 2009.
- [46] H. Narasimha-Iyer, A. Can, B. Roysam, H. L. Tanenbaum, and A. Majerovics, "Integrated analysis of vascular and nonvascular changes from color retinal fundus image sequences," *Biomedical Engineering, IEEE Transactions on*, vol. 54, no. 8, pp. 1436–1445, 2007.
- [47] K. W. Tobin, E. Chaum, V. P. Govindasamy, and T. P.
- [48] Karnowski, "Detection of anatomic structures in human retinal imagery," *Medical Imaging, IEEE Transactions on*, vol. 26, no. 12, pp. 1729–1739, 2007.
- [49] J. Hipwell, F. Strachan, J. Olson, K. McHardy, P. Sharp, and J. Forrester, "Automated detection of microaneurysms in digital red-free photographs: a diabetic retinopathy screening tool," *Diabetic medicine*, vol. 17, no. 8, pp. 588–594, 2000.
- [50] I. Lazar and A. Hajdu, "Microaneurysm detection in retinal images using a rotating cross-section based model," in
- [51] *Biomedical Imaging: From Nano to Macro, 2011 IEEE International Symposium on*. IEEE, 2011, pp. 1405–1409.
- [52] B. Zhang, X. Wu, J. You, Q. Li, and F. Karray, "Detection of microaneurysms using multi-scale correlation coefficients," *Pattern Recognition*, vol. 43, no. 6, pp. 2237–2248, 2010.
- [53] G. Gardner, D. Keating, T. Williamson, and A. Elliott, "Automatic detection of diabetic retinopathy using an artificial neural network: a screening tool." *British journal of Ophthalmology*, vol. 80, no. 11, pp. 940–944, 1996.
- [54] C. Sinthanayothin, J. Boyce, T. Williamson, H. Cook, E. Mensah, S. Lal, and D. Usher, "Automated detection of diabetic retinopathy on digital fundus images," *Diabetic Medicine*, vol. 19, no. 2, pp. 105–112, 2002.
- [55] B. Antal and A. Hajdu, "An ensemble-based system for microaneurysm detection and diabetic retinopathy grading," *Biomedical Engineering, IEEE Transactions on*, vol. 59, no. 6, pp. 1720–1726, 2012.
- [56] X. Zhang and G. Fan, "Retinal spot lesion detection using adaptive multiscale morphological processing," in *Advances in Visual Computing*. Springer, 2006, pp. 490–501.
- [57] L. Tang, M. Niemeijer, and M. D. Abramoff, "Splat feature classification: Detection of the presence of large retinal hemorrhages," in *Biomedical Imaging: From Nano to Macro, 2011 IEEE International Symposium on*. IEEE, 2011, pp. 681–684.
- [58] J. P. Bae, K. G. Kim, H. C. Kang, C. B. Jeong, K. H. Park, and J.-M. Hwang, "A study on hemorrhage detection using hybrid method in fundus images," *Journal of digital imaging*, vol. 24, no. 3, pp. 394–404, 2011.
- [59] R. Phillips, J. Forrester, and P. Sharp, "Automated detection and quantification of retinal exudates," *Graefe's archive for clinical and experimental ophthalmology*, vol. 231, no. 2, pp. 90–94, 1993.
- [60] H. Wang, W. Hsu, K. G. Goh, and M. L. Lee, "An effective approach to detect lesions in color retinal images," in *Computer Vision and Pattern Recognition, 2000. Proceedings. IEEE Conference on*, vol. 2. IEEE, 2000, pp. 181–186.
- [61] M. Niemeijer, M. Abramoff, and B. van Ginneken, "Automatic detection of the presence of bright lesions in color fundus photographs," *Proceedings of IFMBE the 3rd European Medical and Biological Engineering Conference*, vol. 11, pp. 1823–2839, 2005.
- [62] M. Niemeijer, B. van Ginneken, S. R. Russell, M. S. Suttorp-Schulten, and M. D. Abramoff, "Automated detection and differentiation of drusen, exudates, and cotton-wool spots in digital color fundus photographs for diabetic retinopathy diagnosis," *Investigative ophthalmology & visual science*, vol. 48, no. 5, pp. 2260–2267, 2007.
- [63] C. I. Sanchez, R. Hornero, M. I. Lopez, M. Aboy, J. Poza, and D. Abasolo, "A novel automatic image processing algorithm for detection of hard exudates based on retinal image analysis," *Medical Engineering & Physics*, vol. 30, no. 3, pp. 350–357, 2008.
- [64] X. Zhang and O. Chutatape, "Top-down and bottom-up strategies in lesion detection of background diabetic retinopathy," in
- [65] *Computer Vision and Pattern Recognition, 2005. CVPR 2005*.
- [66] *IEEE Computer Society Conference on*, vol. 2. IEEE, 2005, pp. 422–428.
- [67] S. S. A. Hassan, D. B. Bong, and M. Premsenthil, "Detection of neovascularization in diabetic retinopathy," *Journal of digital imaging*, vol. 25, no. 3, pp. 437–444, 2012.
- [68] M. Niemeijer, J. J. Staal, M. Ginneken B. v., Loog, and M. D. Abramoff. (2004) DRIVE: digital retinal images for vessel extraction. [Online]. Available: <http://www.isi.uu.nl/Research/Databases/DRIVE>
- [69]